Proteomic Signature Reveals Modulation of Human Macrophage Polarization and Functions Under Differing Environmental Oxygen Conditions*⑤

Magali Court‡§, Graciane Petre‡§, Michèle EL Atifi‡§, and ⓘ Arnaud Millet‡§¶‖

Macrophages are innate immune cells which can react to a large number of environmental stimuli thanks to a high degree of plasticity. These cells are involved in a variety of tissue functions in homeostasis, and they play essential roles in pathological contexts. Macrophages' activation state, which determines their functional orientation, is strongly influenced by the cellular environment. A large body of macrophage literature is devoted to better defining polarizations from a molecular viewpoint. It is now accepted that a multidimensional model of polarization is needed to grasp the broad phenotype repertoire controlled by environmental signals. The study presented here aimed, among other goals, to provide a molecular signature of various polarizations in human macrophages at the protein level to better define the different macrophage activation states. To study the proteome in human monocyte-derived macrophages as a function of their polarization state, we used a label-free quantification approach on in-gel fractionated and LysC/Trypsin digested proteins. In total, 5102 proteins were identified and quantified for all polarization states. New polarization-specific markers were identified and validated. Because oxygen tension is an important environmental parameter in tissues, we explored how environmental oxygen tension, at either atmospheric composition (18.6% O_2) or "tissue normoxia" (3% O_2), affected our classification of macrophage polarization. The comparative results revealed new polarization-specific makers which suggest that environmental oxygen levels should be taken into account when characterizing macrophage activation states. The proteomic screen revealed various polarization-specific proteins and oxygen sensors in human macrophages. One example is arachidonate 15-lipoxygenase (ALOX15), an IL4/IL13 polarization-specific protein, which was upregulated under low oxygen conditions and is associated with an increase in the rate of phagocytosis of apoptotic cells. These results illustrate the need to consider physicochemical parameters like oxygen level when studying macrophage polarization, so as to correctly assess their functions in tissue. *Molecular & Cellular Proteomics 16: 10.1074/mcp.RA117.000082, 2153–2168, 2017.*

Macrophages are key elements of the innate immune system. Alongside their well-known antiinfection functions, they are involved in numerous homeostatic processes in tissues, including removal of apoptotic cells and remodeling the extracellular matrix (1). Macrophages have been progressively recognized to be involved in systemic metabolism, cold adaptation and development (2). One of the peculiarities of these cells is their phenotypic plasticity (3), which is associated with a broad spectrum of activation states termed polarizations. Polarization is linked to functional phenotypes in specific physiological and pathological processes. A large body of literature related to macrophages is devoted to better defining polarization states from a molecular point of view (4). An M1/M2 dichotomy has been used to present the pro- and anti- inflammatory activation states of macrophages. "Classical" activation, M1, is associated with environments where interferon (IFN)[1]γ and LPS are commonly found. An "alternative" activation, M2 was then recognized, associated with upregulation of the mannose receptor and increased MHC class II expression (5). M2 activation was subsequently subdivided into three states (6): M2a (in response to IL-4 and IL-13), and M2c (induced by IL-10 and/or glucocorticoids or TGF-β) involved in matrix deposition and tissue remodeling; and a third state: M2b (in response to immune complexes

[1] The abbreviations used are: IFNγ, Interferon gamma; ACN, acetonitrile; PBMC, peripheral blood mononuclear cells; DXM, dexamethasone; FDR, false discovery rate; HMDM, human monocyte-derived macrophage; IC, immune complexes; IL, Interleukin; LFQ, label-free quantification; LPS, lipopolysaccharide; MerTK, Mer tyrosine kinase; MFI, median fluorescence intensity; PCA, principal component analysis; QTOF, quadrupole time-of-flight; RT, reverse transcription; TAM, tumor-associated macrophages; TLR, Toll-like receptor.

associated with a TLR agonist), which is implicated in immune regulation (7). This M1/M2 model has been successfully used to describe macrophage responses in multiple situations like acute infections, allergy or obesity (8). Despite this success, this classification has failed to grasp the broad phenotypic repertoire produced by the environmental signals received by macrophages in chronically inflamed tissues or in cancer (9–11). It is now accepted that macrophage activation is best described by a multidimensional model integrating specific microenvironmental signals (12). A recent transcriptome-based network analysis revealed that it was impossible to describe polarization of human macrophages by a dichotomous model like the M1/M2 model (13). The study presented here aimed, among other goals, to provide a molecular signature of various polarizations in human macrophages at the protein level to better define the different macrophage activation states.

Oxygen is an environmental parameter that has gained increasing attention since the recognition of its role in the field of stem cell research (14). Tissue oxygen tension can vary significantly, ranging from 3% to 18.6% O_2, the highest concentrations corresponding to those commonly found in cell culture incubators, and like the oxygen tension encountered by alveolar macrophages. Because alveolar macrophages were found to present functional and morphological differences compared with lung interstitial macrophages (15), it has been hypothesized that the differences are related to the differing levels of oxygen exposure in these tissues (16). Furthermore, bone marrow-derived macrophages exposed to low oxygen levels were shown to present an increased rate of bacterial phagocytosis (16). Oxygen exposure also influenced THP1-differentiated macrophages, although by decreasing phagocytosis (17), it therefore appears that oxygen tension is a fundamental modulator of macrophage polarization that should be clarified at the molecular level in human macrophages.

In the present study, we applied a proteomics approach to address these issues. By measuring expression levels for thousands of proteins simultaneously, we attempted to identify the key molecular differences between different macrophage polarization states under high (18.6%) and low (3%) oxygen conditions. The comparative results revealed new polarization-specific makers which suggest that environmental oxygen levels should be considered when characterizing macrophage activation states. This proteomic analysis highlighted the impact of oxygen on rates of phagocytosis of apoptotic cells, linked to changes in expression levels for proteins such as arachidonate15-lipoxygenase (ALOX15). We could demonstrate that upregulation of ALOX15 is associated with an increase in phagocytosis in IL4/IL13-polarized cells under low oxygen conditions. As clearance of apoptotic cells by macrophages is an essential process in tissue homeostasis, and in the active resolution of inflammation (18), these results demonstrated the importance of molecular characterization of human macrophages to better understand their physiological functions.

EXPERIMENTAL PROCEDURES

Cell preparation and culture—Human blood samples from healthy de-identified donors were obtained from EFS (French national blood service) as part of an authorized protocol (CODECOH DC-2015–2502). Donors gave signed consent for use of their blood in this exploratory study. Peripheral blood mononuclear cells (PBMC) were obtained from whole blood (buffy coat) by density gradient centrifugation (Histopaque 1077, Sigma Aldrich). Monocytes were isolated from PBMCs using CD14 magnetic beads (Miltenyi Biotec) according to the manufacturer's instructions. Purity was assessed by flow cytometry for CD14hiCD45hi cells and found to be > 98%. Monocytes were cultured in RPMI-Glutamax supplemented with 10% human serum AB (Sigma Aldrich) and differentiation was induced by M-CSF (25 ng/ml) over 5 days. Polarization was subsequently obtained by seeding cells in the same concentration of M-CSF and adding specific stimulations for a total of 60 h. Polarization states were induced as follows: M(Ø): no stimulation; M(IFNγ+LPS): IFNγ 10 ng/ml +LPS 1 ng/ml; M(IL-4+IL-13): IL-4 20 ng/ml + IL-13 20 ng/ml; M(IC+LPS): IC + LPS 1 ng/ml; and M(IL-10 + DXM): DXM 10 μM + IL10 25 ng/ml. We used the current convention when describing the polarization induced by the different stimuli, rather than the M1/M2 classification (19). Cells were counted in a Malassez chamber, using trypan blue exclusion to identify live cells. All cytokines and growth factors were purchased from Miltenyi Biotec, France. Dexamethasone (DXM) was purchased from Sigma Aldrich. LPS serogroup 0111 B4 was purchased from Calbiochem. Immune complexes (IC) were obtained by mixing BSA (Bovine serum Albumin from Sigma Aldrich) and antibodies directed against BSA (Invitrogen) at a molar ratio of 1:4 for 1 h at 37 °C before use. Cells were either cultivated under "high oxygen" in an isobaric humidified incubator under 18.6% O_2, 5% CO_2 or under "low oxygen" in an isobaric humidified incubator under 3% O_2, 5% CO_2. For the low oxygen condition, medium was changed in a work station under the same gas conditions to ensure consistent oxygen exposure. Monocytes differentiation starting at day 0 and polarization were performed under the same oxygen condition until cell analysis. Jurkat cells, for phagocytosis assays, were cultured in RPMI with 10% FCS in an isobaric humidified incubator under 18.6% O_2, 5% CO_2.

Proteomics—Cells were directly lysed in Laemmli buffer (234 mM Tris-HCL (pH 6.8), 7.5% SDS, 37% glycerol, 33.3% β-Mercaptoethanol, pinch bromphenol blue). The protein equivalent of 300 000 cells for each sample was loaded on NuPAGE Bis-Tris 4–12% acrylamide gels (Life Technologies SAS). Electrophoretic migration was controlled to allow each protein sample to be split into six gel bands. Gels were stained with R-250 Coomassie blue (Bio-Rad) before excising protein bands. Gel slices were washed three times in 25 mM ammonium bicarbonate (Sigma Aldrich) for 20 min at 37 °C, followed by one wash in (50%/50%, v/v) 25 mM ammonium bicarbonate and acetonitrile (Sigma Aldrich). Gel pieces were then dehydrated with 100% acetonitrile, incubated with 10 mM DTT (Dithiothreitol) in 25 mM ammonium bicarbonate for 45 min at 56 °C, followed by 55 mM iodoacetamide (Sigma) in 25 mM ammonium bicarbonate for 35 min in the dark. Alkylation was stopped by adding 10 mM DTT in 25 mM ammonium bicarbonate. Samples were then washed in 25 mM ammonium bicarbonate and dehydrated with 100% acetonitrile. Proteins were digested overnight at 37 °C with Trypsin/Lys-C Mix (Promega) according to manufacturer's instructions. The resulting peptides were extracted from gel pieces in three sequential extraction steps (each 15 min): 50 μl of 50% acetonitrile, 50 μl of 5% formic acid, and finally 50 μl of 100% acetonitrile. After extraction fractions were pooled and dried in "Mμlti" low-absorption tubes (Dutscher, France) in line with

published recommendations (20). Samples were stored at $-80\ °C$ until further analysis.

Nano-LC-MS/MS Analyses—The dried extracted peptides were resuspended in 2% acetonitrile and 0.05% trifluoroacetic acid (Sigma) and analyzed by online nano-LC (Ultimate 3000, Thermo Scientific) directly linked to an impact II™ Hybrid Quadrupole Time-of-Flight (QTOF) instrument fitted with a CaptiveSpray ion source (Bruker Daltonics, Germany). The flow rate for the nano-LC was set to 400 nL/min. Mobile phases were (A) 0.1% formic acid, 99.9% water; and (B) 0.08% formic acid, 20% water in 79.92% ACN v/v/v. The sample was loaded onto a precolumn (300 μm ID, 5 mm long, 5 μm particles, 100 Å pores Thermo Fisher) during a 5-min injection, peptides were transferred onto a PepMap nano-column (75 μm ID, 50 cm long, 2 μm particles, 100 Å pores, Thermo Fisher) for gradient separation. The gradient profile was: from 2% to 35% B in 115 min; from 35% to 90% B in 5 min; constant 90% B for 10 min before returning to 2% B in 1 min. As a compromise between deep proteome analysis and quantitative analysis, we used a "dynamic method," with a fixed cycle time of 3 s. The mass range of the MS scan was set between m/z 150 and 2200. The duration of dynamic was 30 s. The collision energy was adjusted to between 23 and 65 eV depending on the m/z value.

Analysis of Proteomic Data—All data were analyzed using Max-Quant software (version 1.5.2.8) and the Andromeda search engine (21, 22). The false discovery rate (FDR) was set to 1% for both proteins and peptides, and a minimum length of seven amino acids was set. MaxQuant scored peptide identifications based on a search with an initial permissible mass deviation for the precursor ion of up to 0.07 Da after time-dependent recalibration of the precursor masses. Fragment mass deviation was allowed up to 40 ppm. The Andromeda search engine was used to match MS/MS spectra against the Uniprot human database (downloaded in April 2015, containing 145,892 entries and 245 contaminants). Enzyme specificity was set as C-terminal to Arg and Lys, cleavage at proline bonds and a maximum of two missed cleavages were allowed. Carbamidomethylation of cysteine was selected as a fixed modification, whereas N-terminal protein acetylation and methionine oxidation were selected as variable modifications.

The "match between runs" feature of MaxQuant was used to transfer identification information to other LC-MS/MS runs based on ion masses and retention times (maximum deviation 0.7 min); this feature was also used in quantification experiments. Quantifications were performed using the label-free algorithms (22). A minimum peptide ratio count of two and at least one "razor peptide" was required for quantification.

The LFQ metric was used to perform relative quantification between proteins identified in different biological conditions, protein intensities were normalized based on the MaxQuant "protein group.txt" output (reflecting a normalized protein quantity deduced from all peptide intensity values). Potential contaminants and reverse proteins were strictly excluded from further analysis.

Experimental Design and Statistical Rationale—Three analytical replicates from three independent biological samples (donors) were analyzed for each polarization in the two oxygen conditions, an additional donor was analyzed at 18.6% O_2. For comparisons between pairs of polarizations, only proteins which were quantified in all biological samples in at least one polarization were considered for further processing and statistical analysis. Missing values were deduced from a normal distribution (width: 0.3; down shift: 1.8) using the Perseus (version 1.5.5.3) post data acquisition package contained in MaxQuant (www.maxquant.org). Data were further analyzed using JMP software (v.13.0.0, SAS Institute Inc.). Proteins were classed according to the paired Welch t test difference (difference between the mean value for triplicate MS/MS analyses for the two conditions

compared), and the median fold-change between the two conditions compared. All data are presented as mean ± S.E. Flow cytometry, phagocytosis and qPCR data were analyzed by a paired t test to determine statistical significance of differences between two groups, or by the Tuckey multiple comparison test when more than two groups were compared. All statistical tests were run using GraphPad Prism (v 5.01). The threshold for statistical significance was set to a p value <0.05.

Bioinformatics Analysis—Functional enrichment was analyzed using FunRich (23). Gene Ontology enrichment was determined using DAVID software (https://david.ncifcrf.gov/) (24). A bibliographic search was performed in Pubmed (https://www.ncbi.nlm.nih.gov/pubmed/) and GoogleScholar (https://scholar.google.fr/) for proteins or genes identified as specific for a particular polarization in human monocytes using the following keywords: "macrophages," "polarization," "Human," "Protein name," or "Gene name."

Flow Cytometry—Flow cytometry data was acquired on an Accuri C6 (BD) flow cytometer. The FcR blocking solution (Miltenyi Biotec) was used to prevent nonspecific labeling. The antibodies used were: CD40 FITC (clone HB14), CD14 FITC (clone TÜK4), CD16 PE (clone 3G8, BD Pharmingen), CD206 PE (clone DCN228), CD74 APC (clone 5–239), CD274 APC (clone MIH18), HLA-DR APC (clone AC122) and corresponding isotypic controls (Miltenyi Biotec). Doublet cells were gated out by comparing forward scatter signal height (FSC-H) and area (FSC-A). Dead cells were excluded based on 7AAD or FSC/SSC profile. A least 10,000 events were collected in the analysis gate. Median fluorescence intensity (MFI) was determined using Accuri C6 software (BD).

Immunofluorescence—Cells were cultured on Lab-Tek chambered coverglass (Thermo Fischer). After differentiation and polarization, cells were fixed in paraformaldehyde 4% (Sigma Aldrich) for 10 min. Cells were then permeabilized with Triton at 0.2% for 5 min. Nonspecific binding was saturated by applying BSA 3% for 20 min. A mouse monoclonal antibody directed against STAT1 (Santa Cruz sc-464) was used at 4 $\mu g/ml$, incubated for 1 h at 37 °C. The secondary antimouse Alexa 594 antibody (Invitrogen) was used at 1 $\mu g/ml$, incubated for 45 min at 37 °C. Nuclei were stained with Hoechst 33342 at 1 $\mu g/ml$ (Invitrogen) for 5 min. Images were acquired on a confocal microscope (Fv 10 Olympus) and analyzed using Fiji software (NIH).

Phagocytosis Assay—Apoptosis was induced in Jurkat cells by UV-C ($\lambda = 254$ nm, 7 mW/cm^2) for 5 min. Apoptosis was assessed 16 h after irradiation by flow cytometry based on annexinV-FITC (Miltenyi Biotec) and a 7-AAD (BD bioscience) staining. Three groups of cells were identified: nonapoptotic cells (AnnexinV$^-$ 7AAD$^-$), early apoptotic cells (AnnexinV$^+$ 7AAD$^-$), and late apoptotic cells (AnnexinV$^+$ 7AAD$^+$). Apoptotic cells were stained with TAMRA (5-Carboxytetramethylrhodamine, Sigma Aldrich) and then mixed with macrophage cultures (ratio 5:1) and incubated for one hour. Phagocytosis was assessed by confocal microscopy (Fv 10 Olympus) after staining macrophages with phalloidin-Alexa 488 (Invitrogen) and nuclei with Hoescht 33342 (Invitrogen). Phagocytic events, the number of macrophages containing an apoptotic cell in their cytoplasm, were counted on more than 100 cells per condition using Fiji software. Stock solution (20 mм) of ML351 (Sigma Aldrich) and PD146176 (Sigma Aldrich) were prepared in DMSO. Final solution of DMSO in cell culture medium did not exceed 0.05%. Neither the vehicle nor ML351 or PD146176 modified cell viability. Exposition to ALOX15 inhibitors was performed in parallel to cytokine (IL4, IL13) exposition.

Western Blots—Cell lysates from HMDM were prepared in RIPA with protease inhibitors. Total amount of proteins was determined by BCA Protein Assay kit (Pierce). A volume corresponding to 10 or 20 μg was deposited and run on SDS-polyacrylamide gels according to standard SDS-PAGE protocols. The primary antibodies used were

anti-STAT1 (Santa Cruz sc-464), anti-HK2 (Cell Signaling #2867), anti-ALOX15 (Abcam ab119774) and anti β-actin (Sigma Aldrich) as loading control. Signal was detected by chemoluminiscence (Chemi-Doc Imaging System, Bio-Rad) after incubation with horseradish peroxide-conjugated secondary antibody.

RNA Extraction and RT-qPCR—RNA was isolated from 10^6 cells for each polarization using the MirVana isolation kit™ (Ambion, Applied Biosystems, Foster City, CA). Long RNA and small RNA($<$200 pb) were collected separately. RNA quality and quantity were assessed by performing an Agilent Eukaryote Total RNA Nano assay in a 2100 Bioanalyzer (Agilent Technologies, Santa Clara, CA). Long RNA (400 ng) was transcribed into cDNA using the iScript™ Reverse Transcription (RT) Supermix (BioRad Laboratories, Marnes-la-Coquette, France). The volume of the RT reaction was made up to 100 μl by adding Tris buffer (50 mM, pH 8). For each gene assayed by qPCR, 1 μl duplicate samples were analyzed on a CFX96 Touch™Real-Time PCR Detection System (Bio-Rad), using the SsoAdvanced™Universal SYBR® Green Supermix kit (Bio-Rad). The PCR protocol used was: 3 min at 95 °C; 40 cycles with 15 s at 95 °C and 15 s at 60 °C. PCR primers were designed using the Universal Probe Library Assay Design Center (https://lifescience.roche.com/en_fr/brands/universal-probe-library.html#assay-design-center). The following primers were used: Homo sapiens arachidonate 15-lipoxygenase (ALOX15 NM_001140.3) Forward 5′GCAGCCTGATGGGAAACTC3′ and Reverse 5′GGGGATCCGTAGGCAAGA3′; Homo sapiens ribosomal protein L6 (RPL6 NM_001024662.2) Forward 5′TCCATTCGTCAGAG-CAAACA3′ and Reverse 5′TACGGAGCAGCGCAAGAT3′; Homo sapiens ribosomal protein L27 (RPL27 NM_000988.3) Forward 5′CGCAAAGCTGTCATCGTG3′ and Reverse 5′GTCACTTTGCGG-GGGTAG3′; Homo sapiens WAS protein family, member 2 (WASF2 NM_001201404.2) Forward 5′AAGAAAAGCTGGGACTTCTG3′ and Reverse 5′GCTACTTGCATCCACGTTTTC3′. Relative ALOX15 levels were calculated using the relative standard curve method. Normalization was based on levels of three reference genes, ribosomal protein L6 (*RPL6*), ribosomal protein L27 (*RPL27*) and WAS protein family, member 2 (*WASF2*).

RESULTS

Proteomic Analysis Reveals Proteins Specific for Each Polarization State—To study the proteome in human monocyte-derived macrophages as a function of their polarization state, we used a label-free quantification approach on in-gel fractionated and LysC/Trypsin digested proteins (Fig. 1*A*). In total, 5102 proteins were identified and quantified for all polarization states, with a dynamic range extending over five orders of magnitude according to LFQ (Fig. 1*B*). Principal component analysis (PCA) of differentially expressed proteins revealed specificities in each polarization induced (PC1 30%, PC2 14.6%, PC3 8.9%) (Fig. 1*C*). For macrophages differentiated and polarized under 3% O_2, the PCA analysis showed that M(IFNγ + LPS) and M(LPS+IC) polarizations were very similar in terms of protein expression profile (Fig. 1*C*). Using a fold-change threshold of 2 and a *p* value $<$0.05, we determined the list of proteins overexpressed between two polarizations, as illustrated by volcano-plots representing the comparison between M(IL10+DXM) *versus* M(IFNγ+LPS) at 18.6% O_2 (Fig. 1*D*). A Venn diagram representing overexpressed proteins in the different cases was produced by comparing a polarization to all the other polarizations. A list of proteins specific for each polarization was thus obtained. This analysis provided a list of

specifically overexpressed (Table I in red) or under-expressed (Table I in blue) proteins for each polarization state. For example, 26 proteins were specifically overexpressed in M(IL10+DXM) cells (Fig. 1*E*). Some of these proteins have already been reported as specific for a polarization of HMDM at the protein or mRNA level (supplemental Table S1 and supplemental References). Proteomic identification details for each specific protein can be found in supplemental Table S1 for M(Ø), M(IFNγ+LPS), M(IC+LPS), M(IL4+IL13) and M(IL10+DXM), respectively. Proteomic identification details concerning all identified proteins is present in supplemental Table S2.

Membrane Proteins Expressed on Macrophages as Polarization Markers—Human monocyte-derived macrophages are usually characterized by examining the expression of various surface markers (25). The following surface markers were identified in our proteomics analysis: CD14, CD40, CD74, CD163, CD206, and CD274 (supplemental Fig. S1).These surface markers could be used to identify the different polarizations: M(Ø) as CD14^{hi}CD40^{med}CD74^{med}CD163^{lo}CD206^{lo}CD274^{lo}, M(IFNγ+ LPS) as CD14^{hi}CD40^{hi}CD74^{lo}CD163^{lo}CD206^{lo}CD274^{hi}, M(IC+ LPS) as CD14^{hi}CD40^{hi} CD74^{lo}CD163^{lo}CD206^{lo}CD274^{med}, M(IL4+IL13) as CD14^{lo}CD40^{med}CD74^{hi} CD163^{lo}CD206^{hi} CD274^{med}, and M(IL10+DXM) as CD14^{hi}CD40^{medi}CD74^{med} CD163^{hi}CD206^{hi}CD274^{lo}. Modifying the partial pressure of oxygen under which macrophage differentiation takes place causes modulation of various macrophage functions (17). Nevertheless, no statistically significant differences in levels of surface marker expression were noted in our hand between human macrophage populations grown under 3% and 18.6% O_2. This result was confirmed by flow cytometry analysis of the expression levels of these surface proteins (supplemental Fig. S2). In this analysis, a trend toward increased CD14 expression was noted in all polarization states, except for M(IL4+IL13), and a trend toward decreased CD163 expression was noted for M(IL10+DXM) under low oxygen conditions (*p* = 0.056, paired *t* test, *n* = 18). Taken together, these results suggest that the surface markers commonly used to distinguish between macrophage populations are not sufficiently sensitive to classify changes to macrophage polarization induced by variations in oxygen levels (supplemental Fig. S2).

Proteins Specific for Unstimulated Macrophages—Human monocytes exposed to M-CSF differentiate into macrophages. When no further stimulus is added, these macrophages are considered unstimulated compared with other polarizations. A few proteins were found to be specifically overexpressed in this cellular population. Two candidate proteins were identified: Chitotriosidase-1, which has already been described at the transcriptomic level in M(Ø) macrophages, and cystatin-C (Table I, supplemental Table S1). Some proteins were also found to be specifically under-expressed in M(Ø) compared with other polarizations, these were arachidonate 15-lipoxygenase B (ALOX15B) and Tropo-
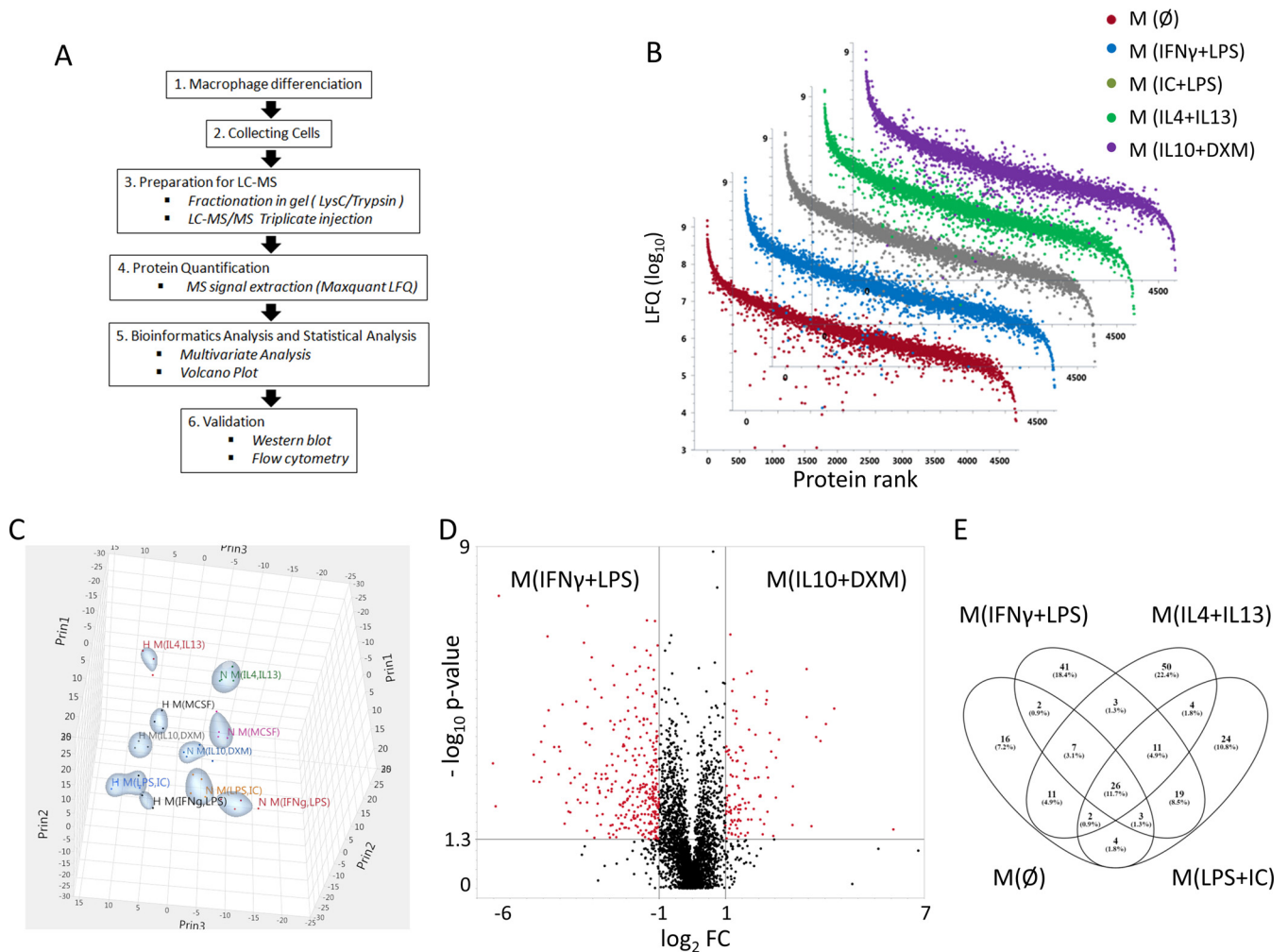
Fig. 1. **Analysis of the proteome of human macrophages.** *A*, Overall experimental workflow. *B*, Rank ordered LFQ for each of the proteins identified (log10 LFQ) in the five polarizations under 18.6% O_2 *C*, 3D graphical representation of the results of a PCA performed on differentially expressed proteins, first three components (ANOVA, $p < 0.05$), for macrophages differentiated under 18.6% or 3% O_2. *D*, Volcano-plots for proteins differentially expressed between M(IL4+IL13) and M(IFNγ+LPS) under 18.6% O_2. Selection criteria were FC > 2 and *p* value <0.05 ($n = 4$ healthy donors). *E*, Venn diagram for M(IL10+DXM) showing that 26 proteins are specific for this polarization compared with all other polarizations at 18.6% O_2.

myosin alpha-3 chain (Table I and supplemental Table S1). ALOX15B is the main element of human 12/15 lipoxygenase and has been described as inducible by multiple stimuli such as IL-4 and LPS (26). Moreover, we found the strongest ALOX15B inducer to be glucocorticoids associated with IL-10 (supplemental Fig. S3) as this protein was identified among the proteins specifically upregulated in M(DXM+IL-10) macrophages (Table I). The low partial pressure of oxygen (3% O_2) by itself did not induce ALOX15B expression, in contrast to reports of expression modulation under extreme hypoxic conditions (0.2% O_2) (26).

M(IFNγ+LPS) and M(IC+LPS) Macrophages Identify a Group of LPS-induced Proteins—Both the PCA analysis (Fig. 1C) and hierarchical clustering indicate that M(IFNγ+LPS) and M(IC+LPS) macrophages are closely related. These polarizations share a common stimulus, the TLR agonist LPS. To

identify the proteins specific to these two polarizations and separate them from LPS-related proteins, we performed a subtractive analysis. This analysis revealed upregulation of proteins mainly implicated in the inflammatory response, as expected (Table II in red, supplemental Table S3). Using DAVID software, the following Gene Ontology (GO) (GO-term)-BP (Biological Processes) were associated with these proteins (Benjamini-Hochberg adjusted *p* value <0.05): immune response, response to virus, cell activation and defense response. These GO-terms were in line with general macrophage function, and were identified in cells grown both under 18.6% O_2 and under 3% O_2. At 3% O_2, the following GO-term was also identified: response to wounding. Analysis of downregulated proteins (Table II in blue, supplemental Table S3) identified MRC1 (CD206; Mannose receptor) a protein known to be associated with alternative activation in human macro-

TABLE I

List of specific over-expressed and under-expressed proteins for each human macrophage polarization

Over-expressed and under-expressed proteins for each polarization obtained through the comparison of each case to all the others are summarized in the table. (GP1B# corresponds to Guanylate binding protein 1; Uniprot accession number Q1D1D5). The proteins in this table are organized by alphabetic order.

	M (∅)		M (IFNγ + LPS)		M (IC + LPS)		M (IL4 + IL13)			M (IL10 + DXM)		
O2 3%	MRPL2	APOL2	MANBA		COII		ACOT7	HSPH1	ACSL1	ACE	LAIR1	ALCAM
	RNF170	APOL3	RNASET2		COX6B1		ALOX15	ITGAM	AGTRAP	AGFG1	NAIP	GPRIN3
		CD274			PARP1		AMPD2	LIMA1	CD14	ALOX15B	PAPSS2	HLA-DRB1
	UPP1	CD38					ARHGAP10	MAOA	FCGR2A	APOD	PLTP	ICAM1
	FKBP5	GBP1#					BTF3	PCM1	TLR2	C1QB	RNASEH2A	NMES1
		GBP5					CD209	PDE6H		C3	SHMT1	RCC2
		HLA-B					CD276	PMVK		CD163	SMAP2	TAOK3
		IDO1					CHCHD2	PPP1R14B		FKBP5	VSIG4	
		NUB1					CRABP2	PSPH		FLOT2		
		PML					DHRS11	PTGS1		FPR1		
		SIK3					EPB41L1	RAB7B		GCA		
		STAT1					EPB41L2	RHOF		GLUL		
		STAT2					FABP4	SCIMP		HMOX1		
		TAP2					HLA-DPA1	SLC27A3		IDH1		
		WARS					HLA-DRA	SLIRP		ITIH1		
							HLA-DRB1	SPN		ITIH4		
							HLA-DRB3	TGM2				
O2 18.6%	CST3	ANKRD22	IDO1	STAT1	HK2		ACOT7	HLA-DRB3	AIF1	ACTC1	NAIP	BID
	CHIT1	APCS	IFITM1	STAT2	TNS1		ALOX15	ITGAM	ALOX5AP	ALOX15B	PAPSS2	DERL1
		APOBEC3	ISG20	STX11	S100A8		ATP1B1	LIMA1	C1QA	APOD	PLTP	DOCK10
		APOL2	LRRK2	TAP2	HDHD1		CD209	MAOA	CD14	C1QA	RABL3	HLA-DRA
	ALOX15B	APOL3	NADK	TMEM41B	SLC2A3		CLUH	MATK	DCTN5	C1QB	SHMT1	HLA-DRB1
	TPM3	CD274	NMI	TOR1B	SEMA6B		CRABP2	PCM1	FCGR2A	C3	ST1A5	ICAM1
		CD38	NUB1	UBE2L6			DHRS11	PIEZO1	FDX1	CD163	TWF1	IL4I1
		CYB5A	PARP10	VAMP5			EPB41L2	PLCB2	IL18	CD302	VSIG4	MYL12A
		DHX58	PDE6D	WARS			EVL	PTGS1	LAIR1	F13A1	WDR26	NUP93
		DPYD	PVRL2		AMDHD2		FN1	RAB7B	RAB27A	FCGR2A		PLAUR
		FAM49A	RAB7L1		COII		FRMD4A	SLC6A6	SIGLEC1	FKBP5		PLIN2
		FSCN1	RILPL2				GHITM	SORT1	TLR2	FPR1		PTDSS1
		GBP1#	RNF114				HAAO	SPN		GLUL		RAB7B
		GBP4	SEMA4A				HLA-DPA1	TGM2		HMOX1		SET
		GBP5	SLC2A6	RNASET2			HLA-DPB1	TIMMDC1		HSP90AB4P		TNFAIP8L2
		GCH1	SLC30A1	TFRC			HLA-DPB1			LAIR1		ZFYVE16
		HLA-C					HLA-DRB1			METTL7A		

phages (6). Indeed, CD206 is a surface protein mainly expressed in M(IL4+IL13) and M(IL10+DXM) macrophages (supplemental Fig. S1), and this expression pattern was confirmed by flow cytometry (supplemental Fig. S2).

Proteins Associated with IFNγ/LPS Activation—Proteins specifically upregulated in M(IFNγ + LPS) irrespective of oxygenation conditions were: Apolipoprotein L2 (APOL2), Apolipoprotein L3 (APOL3), Indoleamine 2,3-dioxygenase 1 (IDO1), Guanylate binding protein 1, Guanylate binding protein 5 (GBP5), Programmed cell death 1 ligand 1 (CD274), Signal transducer and activator of transcription 1-alpha/beta (STAT1), Signal transducer and activator of transcription 2 (STAT2), Tryptophan-tRNA ligase (WARS), and Antigen peptide transporter 2 (TAP2) (Table I). All these proteins have already been reported in human macrophages at the protein or mRNA level (supplemental Table S1). Two proteins emerged as candidate new markers of human M(IFNγ + LPS): NEDD8 ultimate buster 1 and ADP-ribosyl cyclase/cyclic ADP-ribose hydrolase 1 (CD38) which previously had only been reported to be induced by LPS in murine macrophages (27). The transcription factor STAT1 has been described as a key molecular component of the IFN-γ response of macrophages (19). When IFNγ binds to its receptor at the cell membrane, it induces phosphorylation of STAT1 by members of the JAK (Janus kinase) family of protein tyrosine kinases. p-STAT1 in a homodimer or a heterodimer with STAT2 then translocates to the nucleus where it induces transcription of target genes (28). Our label-free quantification approach revealed that overall expression of STAT1 is upregulated in M(IFNγ + LPS) macrophages (Fig. 2A), as it has been previously reported at 18.6% O2 (29) but also that 3% O2 exposure does not modify this expression. This result was confirmed by Western blotting analysis of M(IFNγ + LPS) samples; STAT1 was also detected by Western blotting at lower levels in M(IC + LPS), but it was undetectable in other polarizations (Fig. 2B) and in unpolarized macrophages (data not shown). Overexpression of STAT1 was also confirmed by confocal microscopy and demonstrated its nuclear localization (Fig. 2C).

TABLE II

List of specific over-expressed and under-expressed proteins for macrophages exposed to LPS

Over-expressed and under-expressed proteins related to the exposure to LPS were obtained after a subtractive analysis to eliminate specific proteins of M(IFNγ+LPS) and M (IC+LPS) macrophages. The proteins in this table are organized by alphabetic order.

	M (IFNγ + LPS) and M(IC + LPS)				
O₂ 3%	ADA	hsOAS3	NCF1	SERPINB9	DAB2
	AKR1B1	ICAM1	NFKB1	SOD2	FEX1
	ALAS1	IFIT1	NFKB2	STAT3	GATM
	AMPD3	IFIT2	NMES1	TAP1	GLG1
	CD40	IFIT3	NR3C1	TAPBP	GUSB
	CD48	IL18	OAS2	TNFAIP2	HMOX1
	CD82	IL4I1	PARP9	TNFAIP8	LIPA
	CLIC4	ISG15	PILRA	TOM1	LRPAP1
	CMPK2	ISG20	PLAUR	TRG14	METTL7A
	DDX58	ITGAL	PLSCR1	TRIP10	MRC1
	DTX3L	KYNU	PSTPIP2		SDCBP
	EIF2AK2	LYN	PTAFR		
	GBP2	MARCKS	RDX		
	GRAMD1A	MX1	RIPK2		
	HLA-A	MX2	RNF213		
	HLA-C	MYH11	SAMD9		
O₂ 18.6%	ALAS1	IFIT3	NT5C3	TAPBP	ACE
	CD48	IFIT5	OAS1	TNFAIP2	DAB2
	CD82	IL18	OAS2	TRG14	LIPA
	CKB	IL4I1	PILRA	TRIP10	MRC1
	CLIC4	ISG15	PLAUR	TXN	PPT1
	CMPK2	ISG20	PLSCR1	ZNRF2	
	DDX58	ITGAL	PSTPIP2		
	DOCK4	KYNU	PTAFR		
	EIF2AK2	LYN	RELB		
	FMNL2	MARCKS	RILPL2		
	GBP2	MX1	RNF213		
	GRAMD1A	MX2	SAMD9		
	HLA-A	MYH11	SAMD9L		
	hsOAS3	NCF1	SERPINB9		
	ICAM1	NFKB2	SOD2		
	IFIT1	NMES1	SRXN1		
	IFIT2	NR3C1	TAP1		

In M(IL-4 + IL-13) macrophages, STAT1 is expressed at lower levels and no nuclear localization was detected (Fig. 2C). These results indicate that IFNγ stimulation of macrophage is associated with an increased overall expression of intracellular STAT1 60 h after the start of the stimulation. We also found that STAT1 is localized in the nucleus, which is known to occur when this transcription factor is phosphorylated, demonstrating that this overexpression is functional (30). Our results indicate that the STAT1 molecular pathway is unaffected by reduced oxygen levels, as no differences were visible between 18.6 and 3% O₂ conditions (Fig. 2A and 2B). A similar result was found for STAT2 using LFQ analysis (data not shown).

Analysis of the Phenotype Induced by Immune Complexes and LPS—Despite sharing LPS stimulation with M(IFNγ + LPS) macrophages, proteins specific for M(IC+LPS) macrophages were identified (Table I, supplemental Table S1): hexokinase-2 and a glucose transporter, SLC2A3 (supplemental Table S1). Hexokinase-2 is involved in the first step of glycolysis and has been described as elicited by LPS-driven reprogramming of "inflammatory" macrophages toward a glycolytic energy source (31). This protein is also upregulated in M(INFγ+LPS) macrophages compared with other polarization states studied here (Fig. 3A and 3B). This result confirms the glycolytic signature of human "M1" macrophages when activated by LPS (32). This result indicates that the metabolic signature generally used to distinguish classically activated and alternatively activated macrophages is incompatible with the oxygen environment found in a majority of human tissues. The modulatory role of this polarization is illustrated by the lower expression of the STAT1 transcription factor compared with M(IFNγ + LPS) (Fig. 2A and 2B).

Alternative Activation Induced by IL4/IL13—M(IL4+IL13) are classed as anti-inflammatory cells. Our results support this classification as TLR2 and CD14, implicated in the TLR4-mediated response to LPS (33), are downregulated (Table I). This polarization is characterized by the overexpression of
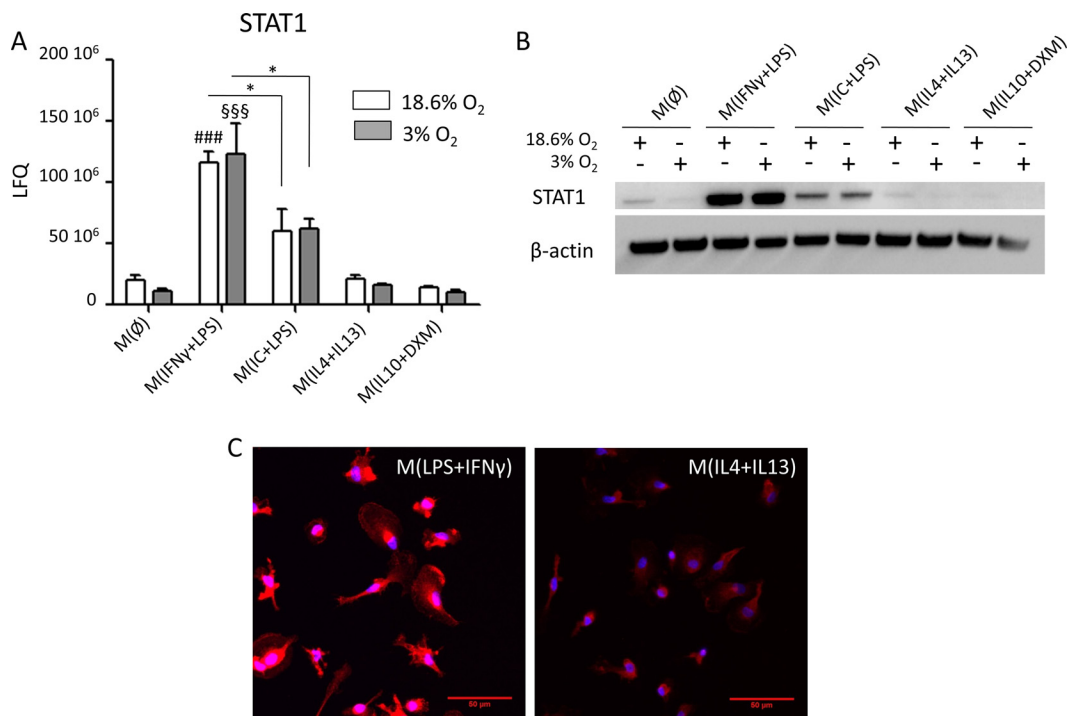
FIG. 2. **STAT1 transcription factor expression increases in M(IFNγ+LPS) macrophages and locates to the nucleus.** A, Expression of STAT1 determined by LFQ on mass spectrometry data ($n = 4$ for 18. 6% O_2, $n = 3$ for 3% O_2). B, Western blotting analysis of STAT1 expression in total cell lysates of macrophages cultured under 18.6 and 3% O_2. 20 μg of protein was deposited in each well. Loading control was based on β-actin levels. Results shown are representative of four independent experiments. C, Validation and localization of STAT1 expression using a non phosphospecific antibody in M(IFNγ+LPS) and M(IL4+IL13) macrophages by immunofluorescence. STAT1 overexpression in the M(IFNγ+LPS) condition is associated with a nuclear localization. Results shown are representative of three independent experiments performed under 18.6% O_2.

FIG. 3. **The glycolytic signature of LPS-exposed macrophages is lost under low environmental oxygen tension.** A, Hexokinase-2 expression levels (LFQ) in all polarizations under 18.6 and 3% O_2 exposure. Hexokinase-2 is induced in LPS-stimulated macrophages, M(IFNγ+LPS) and M(IC+LPS), compared with non-LPS-stimulated polarizations in high oxygen conditions (§§ $p <$ 0.01 for M(IFNγ+LPS) and ## $p < 0.01$ for M(IC+LPS) Tuckey's multiple comparison test, * $p < 0.05$ Tuckey's multiple comparison test, ** $p < 0.01$, ***$p <$ 0.001 Welch paired t test). B, Western blotting analysis of Hexokinase-2 expression in total cell lysates of macrophages cultured under 18.6 and 3% O_2. 10 μg of protein was deposited in each well. Loading control was based on β-actin levels.
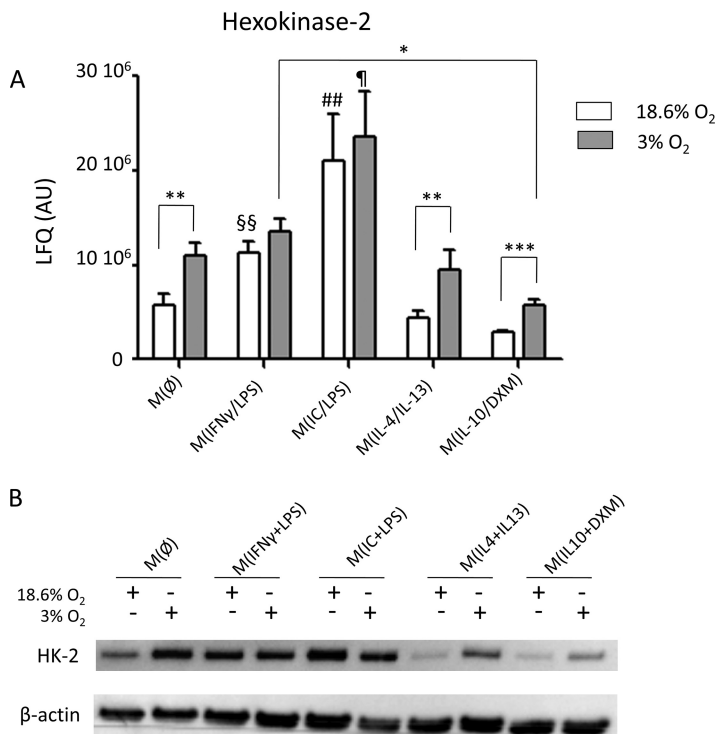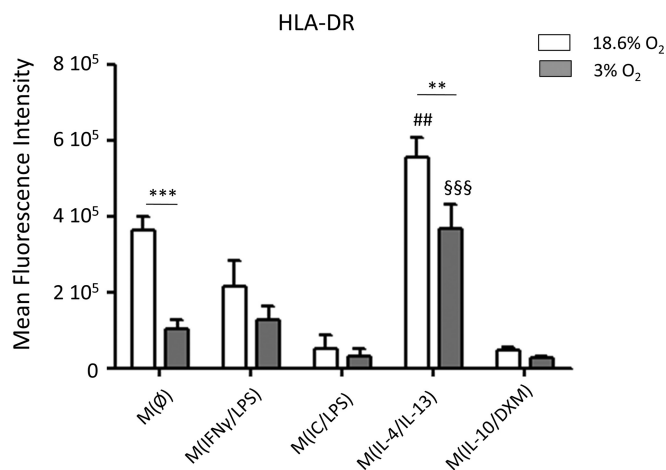
Fig. 4. **Flow cytometry analysis of HLA-DR expression under low oxygen tension.** HLA-DR is mainly expressed at the surface of M(IL4+IL13) macrophages (## $p < 0.01$ 001 Tuckey's multiple comparison test at 18.6% O_2, §§§ $p < 0.001$ Tuckey's multiple comparison test at 3% O_2). Expression of this protein is downregulated in low oxygen conditions for M(IL4+IL13) macrophages (** $p < 0.01$, paired t test) and for M(Ø) (*** $p < 0.001$, paired t test). These results were obtained from 12 independent healthy donors.

many MHC class II proteins: HLA-DRA, HLA-DRB1, HLA-DRB3, HLA-DPA1 and HLA-DPB1 (Table I, supplemental Table S1). CD74, which helps guide the CD74-MHC-II complex to the endolysosomal compartment is also upregulated in these macrophages, although the level of change was not statistically significant in LFQ (supplemental Fig. S1). The result was nevertheless confirmed by flow cytometry (supplemental Fig. S2). This MHC II expression was further investigated by flow cytometry analysis of the different HLA-DR molecules (Fig. 4), and once again the 3% O_2 condition was associated with a strong downregulation of HLA-DR in M(Ø) macrophages, and to a lesser extent in M(IL4+IL13) macrophages (supplemental Fig. S4). The downregulation of HLA-DRB1, HLA-DRB3 and HLA-DRA in M(Ø) at 3% O_2 was confirmed by our LFQ analysis (data not shown).

General Response to Decreased Partial Pressure of Oxygen in Human Macrophages—Hierarchical clustering of differentially expressed proteins was used to classify polarization states (Fig. 5). This analysis revealed four main protein clusters related to LPS-stimulated, IL4/IL13-stimulated, and IL10/DXM-stimulated macrophages, as well as a cluster of proteins overexpressed in all polarizations on exposure to 3% O_2 (supplemental Table S4). To determine the molecular pathways with which these proteins are mainly associated, we performed a FunRich enrichment analysis of the biological pathways involved in this cellular response to a low-oxygen environment (Fig. 6A). The main categories of biological pathways identified were: metabolism, mitochondrial citric acid cycle, respiratory electron transport, glycolytic metabolism and HIF-1α network. In a complementary analysis, we used the GO-BP (Biological Processes) analysis available in DAVID

software (Fig. 6B). Glycolytic processes and respiratory electron transport were the main biological processes associated with the proteins induced under low oxygen conditions. These results describe the general macrophage response to a low-oxygen environment, which corresponds to "normoxia" in many tissues. This response involves many overexpressed proteins under the control of the transcription factor HIF-1α and the reorientation of the cellular metabolism toward glycolysis.

The "M1/M2 Dichotomy" Under Low Partial Pressure of Oxygen—The M1/M2 dichotomy is often used to compare pro- and anti-inflammatory activation states of macrophages. This dichotomy equates M1 to IFNγ-stimulated macrophages ($\pm$ LPS) and M2 to IL4-polarized macrophages, possibly associated with IL13 (6). To characterize this classification using our proteomics approach, we used an enrichment of GO-terms-BP analysis of overexpressed proteins in the M(IFNγ+LPS) and M(IL4+IL13) samples at 3% compared with 18.6% O_2 (supplemental Fig. S4). M(IFNγ+LPS) macrophages were mainly involved in the antiviral response and inflammatory response mediated by the IFNγ signaling pathway. In contrast, M(IL4+IL13) macrophages were associated with antigen presentation through MHC class II molecules. A similar profile of biological process enrichment was observed when macrophages were exposed to a low-oxygen environment, although some new GO-terms appeared at 3% O_2. IFNγ/LPS polarization was associated with the following terms: antigen presentation via TAP-independent MHC class I, positive regulation of nitric oxide biosynthetic process, positive regulation of interleukin-6 production, leukocyte migration and response to hypoxia (supplemental Fig. S4A). IL4/IL13-polarized macrophages at 3% O_2 also had new GO-terms, mainly in categories associated with MHC class II-mediated antigen presentation, as well as translation and transcription regulation and response to hypoxia (supplemental Fig. S4B).

Polarization-specific Proteins as Sensors of Environmental Oxygen—Proteins specific for a particular polarization that maintain their specificity regardless of oxygen levels could nevertheless display modulations in expression levels between 3% and 18.6% O_2 (FC > 2, paired Welch t test $p < 0.05$), making these proteins candidate polarization-specific oxygen sensors. The following proteins fulfill these criteria for M(IL4+IL13) macrophages: ALOX15 (Arachidonate 15-lipoxygenase), CRABP2 (Cellular retinoic acid-binding protein2), both of which are upregulated at 3% O_2; HLA-DPA1 and CD209 (DC-SIGN) which are downregulated at 3% O_2. A single protein was found upregulated at 3% O_2 for M(IL10+DXM) macrophages: NAIP (Baculoviral IAP repeat-containing protein 1).

Macrophage Phenotype Induced by IL10 and Corticosteroids—Proteomic (supplemental Fig. S1) and flow cytometry (supplemental Fig. S2) analyses clearly confirmed overexpression of the well-known scavenger receptor CD163 in M(IL10+DXM) macrophages. Proteomic analysis also confirmed other previously reported markers such as FPR1
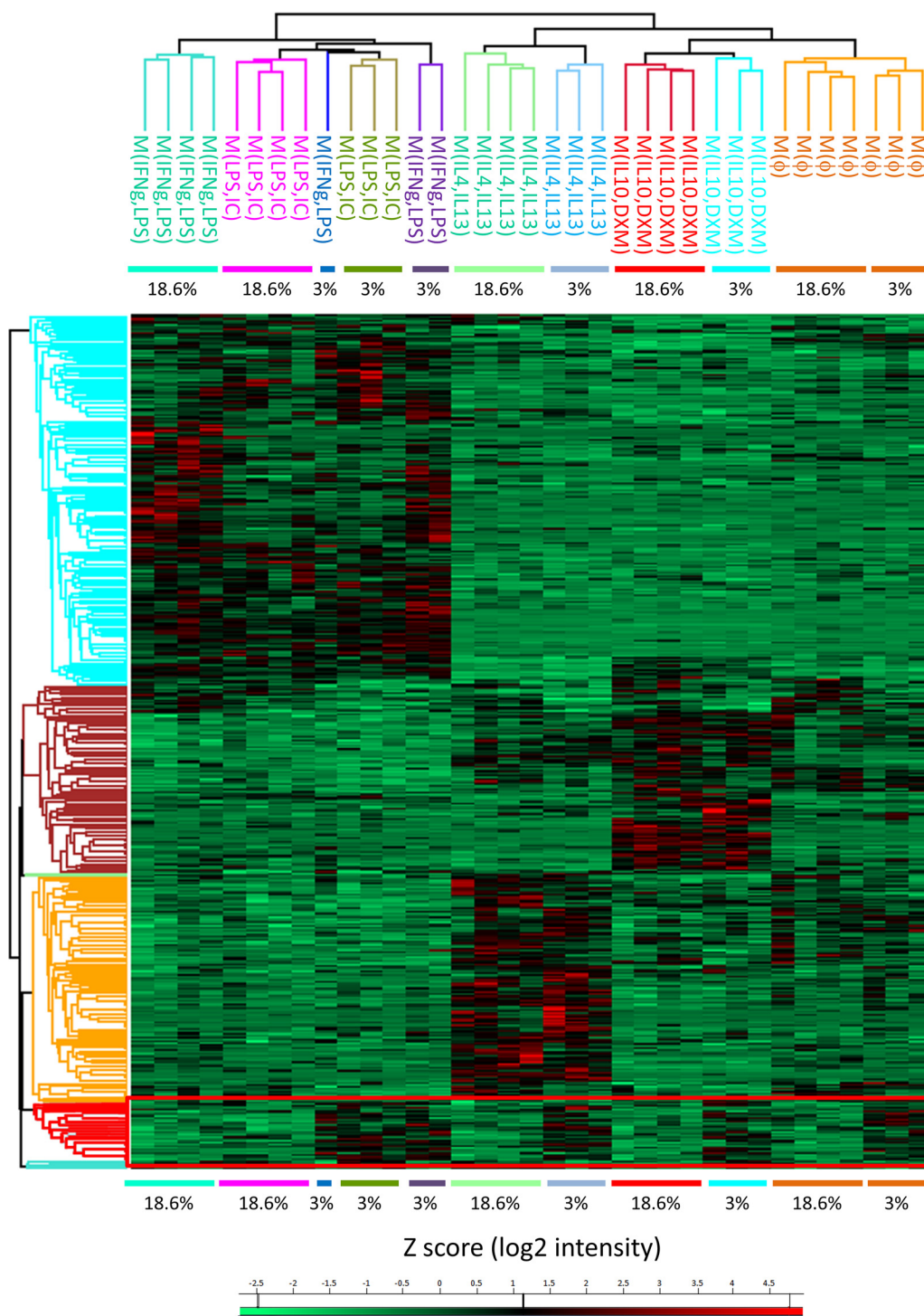
FIG. 5. **Classification of polarization of human macrophages.** Heat-map representing the hierarchical clustering of all polarization states using differentially expressed proteins. Analysis reveals a cluster of proteins overexpressed in all polarizations in the 3% O_2 condition (red rectangle). The color scale represents Z-Score (log_2 intensity). Each row is a protein and each column is a sample.

(Formyl peptide receptor 1), VSIG4, coagulation factor XIII and FcγRIIa (CD32) (Table I, supplemental Table S1). MHC II molecules (HLA-DRB1, HLA-DRA) were downregulated in this polarization (Table I) along with some HLA-associated proteins like TAPBP, SET and DERL1 (supplemental Table S1).

Increased Clearance of Apoptotic Cells by M(IL4+IL13) Under Low Oxygen Conditions is Related to Overexpression of ALOX15—Our proteomic analysis revealed that ALOX15 is specifically expressed in M(IL4+IL13) macrophages, with significantly increased expression at 3% O_2 (Fig. 7A). We could
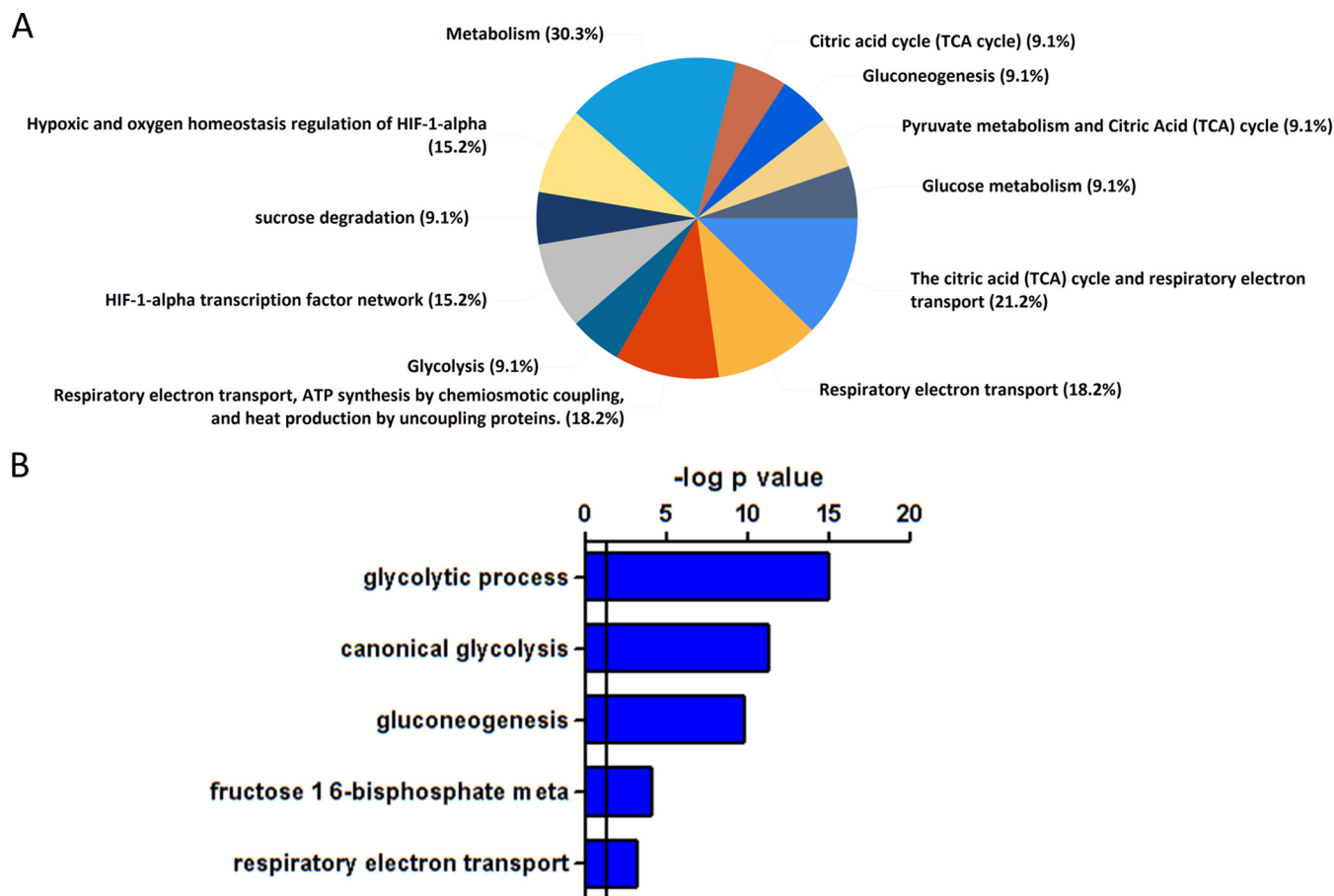
A

B

FIG. 6. **Overall response of human macrophages to low oxygen tension.** Enrichment analysis of proteins overexpressed in all polarization states in low oxygen conditions. *A*, A FunRich analysis was performed to identify which biological pathways were affected in low oxygen conditions (p value adjusted with Benjamini-Hochberg procedure <0.05). *B*, GO-term (Biological Processes) enrichment was performed on these proteins using DAVID software (p value is used for the graphical representation, the main GO-Term was selected on the adjusted p value by applying Benjamini-Hochberg procedure <0.05).

confirm this pattern of expression by Western blotting analysis (Fig. 7*B*). We found that this expression was regulated at the transcriptomic level as the ALOX15 mRNA expression determined by qPCR at 18.6% O_2 was 843.3 ± 205.1 (AU) *versus* 5936 ± 1905 (AU) at 3% O_2 ($p < 0.05$, paired t test $n = 5$). ALOX15 mRNA levels were undetectable in other polarizations. We found that ALOX15 is implicated in the ability of M(IL4+IL13) macrophages to phagocyte apoptotic cells using. Using ML351 and PD146176, which are known specific inhibitors of ALOX15 activity (34), we were able to show that this inhibition significantly decrease the phagocytosis rate of macrophages (Fig. 7*C*). We then could show that exposure to low oxygen levels, which is associated with an induction of ALOX15 expression, did increase significantly M(IL4+IL13) macrophages efferocytic abilities (Fig. 7*D*). This low oxygen exposition was not associated with an altered rate of phagocytosis of apoptotic cells in other polarization (Fig. 7*D*). This result illustrates how the phagocytic capacity of polarized macrophages could be altered in response to environmental variables like oxygen tension, even in the presence of polarizing biochemical signals.

C1q is Specific for M (IL10 + DXM) Macrophages, and Associated with Extensive Phagocytosis of Apoptotic Cells— C1q is a component of the complement cascade which has been implicated in the phagocytosis of apoptotic cells (35). One of the receptors associated with the C1q-dependant phagocytosis of apoptotic cells is MerTK (mer tyrosine kinase), a member of the TAM (Tyro3, Axl, Mer) family of receptors (36). It has been suggested that MerTK is overexpressed in response to IL10 stimulation, and that this could explain the higher capacity of M(IL10) macrophages to internalize apoptotic cells (36). Our results confirmed that M(IL10+DXM) macrophages display a higher rate of phagocytosis of apoptotic cells compared with other polarizations in hyperoxic conditions (Fig. 7*D*). This high rate of phagocytosis is also associated with a high phagocytic index, translating the mean number of apoptotic cells internalized by a single macrophage. In M(IL10+DXM) macrophages, this index was greater
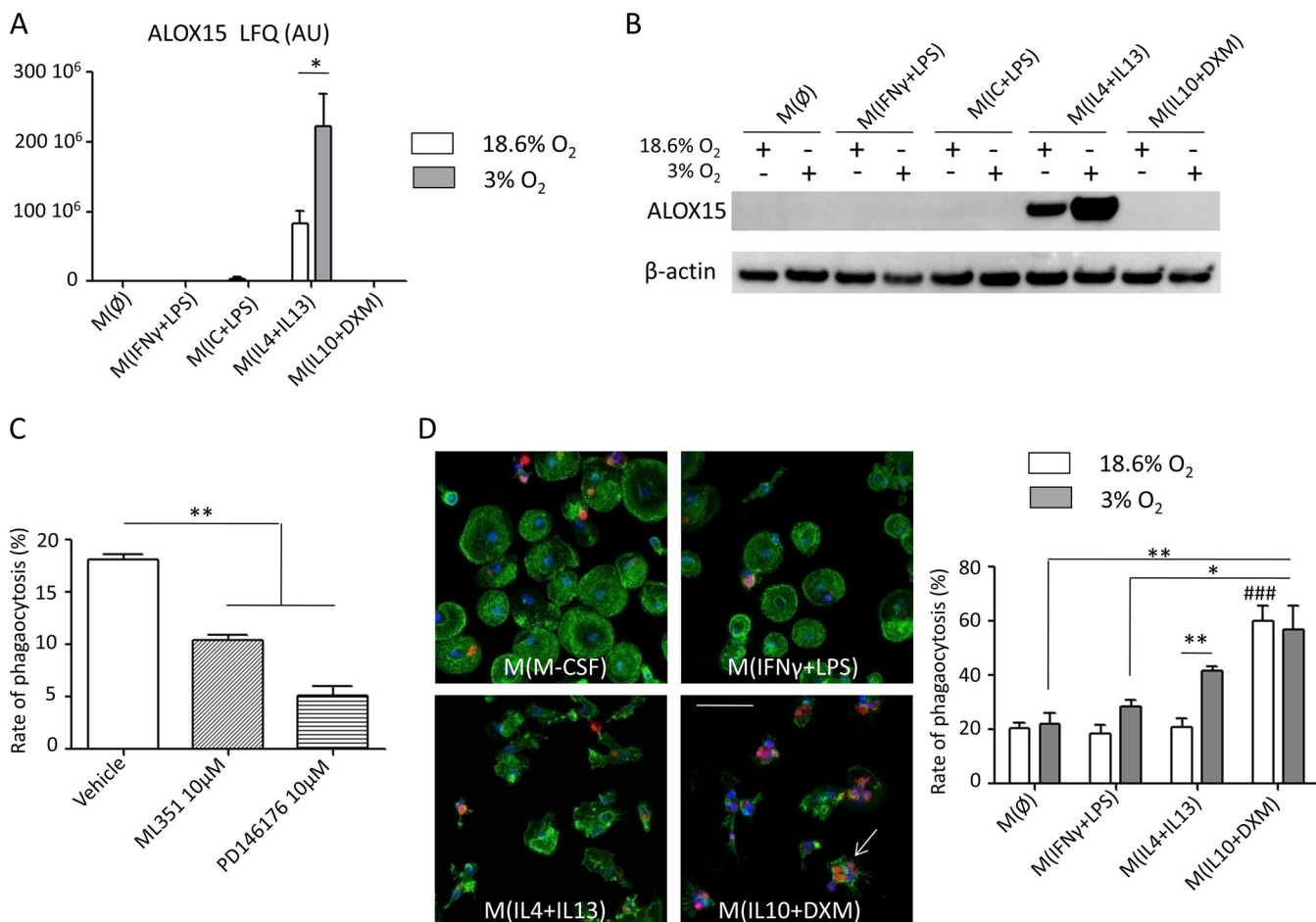
FIG. 7. **Upregulation of ALOX15 increases the phagocytic capacity of M(IL4+IL13) macrophages in a low-oxygen environment.** *A*, ALOX15 is specifically expressed in M(IL4+IL13) in low oxygen conditions (**$p < 0.01$, t test). *B*, Western blotting validation of the expression of ALOX15 which is only found in M(IL4+IL13) and induced in low oxygen condition. 10 μg of protein was deposited in each well. Loading control was based on β-actin levels. *C*, ALOX15 is a lipo-oxygenase implicated in the phagocytosis of apoptotic cells as it is demonstrated by the decrease in phagocytosis rate of M(IL4+IL13) when macrophages are exposed to specific inhibitors of ALOX15 activity ML351 and PD146176 (** $p < 0.01$, t test $n = 3$ independent experiments). *D*, Immunofluorescence analysis of the phagocytosis of apoptotic Jurkat (red = stained by TAMRA) by human macrophages (blue = Hoescht staining of nucleus, green = phalloidin-Alexa488). Scale bar corresponds to 50 μm. Quantification of phagocytosis (### $p < 0.001$ for comparison between M(IL10+DXM) and all other polarizations at 18.6% O_2; * $p < 0.05$,**$p < 0.01$, paired t test $n = 3$ independent experiments).

than 1, whereas in other polarizations only one apoptotic cell was visible in each macrophage engaged in efferocytosis. This phagocytic phenotype is associated with overexpression of MerTK in M(IL10+DXM) macrophages, and expression of C1q by the macrophages themselves (supplemental Fig. S5). Thus, M(IL10+DXM) phagocytic capacity is probably linked to the MerTK-C1q pathway, with both of these proteins synthesized by macrophages. C1q by itself has also been shown to induce the expression of MerTK (36). We could demonstrate that M(IL10+DXM) maintain their phagocytic capacity at 3% O_2 (Fig. 7D), and that C1q expression was unaffected by changes to the environmental oxygen tension (supplemental Fig. S5).

DISCUSSION

Macrophages form a group of specialized innate immune cells found in all tissues. The ontogeny of these cells is complex, and tissue-resident macrophage populations could originate in the yolk sac, the fetal liver or the bone marrow (12). Circulating monocyte-derived from bone marrow progenitors not only replenish some tissue-resident macrophage compartments (*e.g.* gut macrophages) but could be recruited by various tissues in response to sterile or infection-related inflammation leading to their differentiation into macrophages. This differentiation takes place under the influence of multiple signals (*e.g.* cytokines, chemokines, growth factors and danger signals) which lead to partially reversible polarization (1). Depending on the type of cytokines present in the tissue microenvironment, in particular those secreted by T helper lymphocytes, it is common to describe a "classical" activation (M1) under the control of interferon-γ (that may be associated with LPS) and an "alternative" activation (M2a) induced by IL-4/IL-13. This classification, although useful, was rapidly

found to be inadequate to grasp the continuum of activation states observed *in vivo* (6).

Macrophage activation states are related to strong functional differences in their secretome, their ability to synthesize and remodel the extracellular matrix and their phagocytic capacities. Transcriptomic analysis has revealed a huge number of potential biomarkers associated with a polarization (13, 37, 38). This approach also revealed important markers such as tranglutaminase 2 (TGM2) for IL-4 polarized macrophages (39), and the partially shared transcriptomic profile between human and murine macrophages (39). Less work has been performed at the proteomic level on human macrophages, and comparison with transcriptomic data indicated only limited comparability between gene and protein levels (39). There is therefore a clear need to explore the proteome of human macrophages in various polarization states to determine a molecular signature and relate it to functional phenotypes. Because most tissues where monocytes undergo differentiation present an environmental oxygen tension sometimes far below the atmospheric one, we decided to study how this physicochemical parameter affected human macrophage polarization. The influence of oxygen on macrophage phenotypes is illustrated by differences reported between alveolar macrophages and lung interstitial macrophages (15). These morphological and functional differences are believed to be related to the differing oxygen levels in which these two cell categories are found (16). Phagocytosis of bacteria has been shown to increase in murine bone marrow-derived macrophages when exposed to low levels of oxygen (16), and an opposite result was found in human THP1-differentiated macrophages (17). These results illustrate the need to understand how oxygen modulates macrophage polarization and functions.

Macrophage differentiation and polarization involves a range of metabolic pathways. LPS-activated macrophages are associated with a glycolytic profile, whereas IL-4 macrophages tend to use oxidative phosphorylation and the Krebs cycle to produce ATP (40). Our results indicate that human macrophages are also effectively associated with a glycolytic profile when exposed to LPS, as in the case of M(IC+LPS) and M(IFNγ+LPS) macrophages. Hexokinase-2, which is involved in the first step of glycolysis, was identified as one of the overexpressed proteins in both polarizations (Fig. 3*A* and 3*B*). This protein is strongly related to the "Warburg effect," or aerobic glycolysis (41). In addition to hexokinase-2, a similar expression profile was found for SLC2A3 (Solute carrier family 2, facilitated glucose transporter member 3) a glucose transporter (data not shown). This result confirms the LPS-driven metabolic reprogramming toward aerobic glycolysis under 18.6% O_2. Because low O_2 exposure is associated with a switch toward anaerobic glycolysis, we studied how exposure to lower oxygen levels modifies this metabolic signature. Even though 3% O_2 exposure does not represent profound hypoxia, but rather "tissue normoxia," we found that all polar-izations were associated with the induction of HIF-1α-related genes, and their metabolic profiles were oriented toward glycolysis (Fig. 6*A* and 6*B*). We also found that the metabolic reprogramming of LPS-stimulated macrophages was lost under 3% O_2, as Hexokinase-2 was no longer specific to LPS-stimulated macrophages. Indeed, its expression was increased in all polarizations in these conditions (Fig. 3). Metabolism in IFNγ/LPS-stimulated macrophages was also associated with overexpression of DPYD (Dihydropyrimidine dehydrogenase [NADP(+)]) (Table I, supplemental Table S1), a protein implicated in pyrimidine catabolism. This specific expression related to IFNγ/LPS was lost when differentiation took place at 3% O_2 (Supplemental Table S2). This protein appears to be a good low-oxygen sensor in macrophages whatever their polarization (supplemental Fig. S6). DPYD is known to degrade 5-Fluorouracil (5-FU), a standard chemotherapy drug. Overexpression of this protein by cancer cells has been linked to resistance to this treatment in cancer patients (42). Because tumor-associated macrophages (TAM) evolve in a low-oxygen environment, our results suggest that these cells could be implicated in resistance to 5-FU if they express high levels of DPYD, opening the possibility to design a DPYD inhibitor-based therapeutic strategy to target macrophages.

Since the seminal work of Janeway *et al.* (43), it is demonstrated that an inadequate low number of MHC class II molecules at the surface antigen presenting cells would lead to a decreased antigen presentation. In our results we found that M(IL4+IL13) macrophages present a downregulation of the expression of HLA-DR at their surface when exposed to low oxygen condition (Fig. 4). This effect was also found for M(Ø) macrophages. The mechanism by which low oxygen downregulates the expression of MHC class II molecules is not known. Despite this fact, it has been demonstrated that during the 24 h following a shock/trauma (especially when hemorrhagic), macrophage expression of CMH II molecules and their capacity to present antigen is decreased associated with the cell's metabolic response to regional hypoxia (44). The main consequence of the downregulation of MHC II molecules in macrophage exposed to low oxygen environment is the protumoral role of tumor associated macrophages (TAM). In tumor mice models it has been demonstrated that low MHC-II expression macrophages populate hypoxic areas whereas TAMs with high MHC-II expression are found in normoxic areas (45). In a mouse lung carcinoma model it has been reported that MHC-II low macrophages express M2 markers such as mannose receptor or IL4-Rα (46). Our results reinforce the importance of considering low oxygen environment impact on M(IL4+IL13) macrophage through MHC-II molecules expression and immune-tolerance in a tumoral context. Under exposition to low oxygen M(IL4+IL13) macrophages also down regulate their level of expression of DC-SIGN (CD209) even if this protein is still only expressed in this polarization. DC-SIGN is a type II transmembrane C-type

lectin with a carbohydrate recognition domain. *In vitro* this protein is induced by M-CSF and IL-4 (37). *In vivo* this protein, expressed on macrophages, has been implicated in the inhibition of T-cell proliferation and induction of the expansion of Foxp3+ Treg (47). DC-SIGN appears as an element maintaining an immunosuppressive tissue environment favoring immune escape of tumors (48), but is also a receptor of various pathogens notably in alveolar macrophages. The downregulation of this protein under low oxygen in macrophage modulates the expected immune-suppressive phenotype associated with MHC-II molecules downregulation. It could also be understood, in a inflammatory context associated with hypoxia, as a controlled downregulation of a receptor used by pathogens like mycobacteria to infest alveolar macrophages (49). M(IL4+IL13) macrophages are also associated with the upregulation of the expression of CRABP2 under low oxygen, this protein is implicated in the transport of retinoic acid to nucleus. Even if it needs further investigation the retinoic acid signaling is of uttermost importance in macrophage biology, for example it has been demonstrated that retinoid X receptor alpha deficient mice are associated with an autoimmune nephritis produced by a defect of the clearance of apoptotic cells by macrophages (50). Genes implicated in the clearance of apoptotic cells have their expression impaired in these mice: *CD36*, *MERTK*, *C1Q* and *TGM2*. Our results also show that M(IL10+DXM) macrophages present an upregulation of NAIP expression under low oxygen exposure. This protein acts as a sensor component of the NLRC4 inflammasome (51) specific to intracellular bacteria leading to the activation of caspase-1. Lowering oxygen dispensability in a tissue appears to be sense by these macrophages as an inflammatory signal.

Our proteomic approach identified several proteins known to be implicated in efferocytosis, the phagocytosis of apoptotic cells. This process is a specific function of macrophages for the maintenance of normal and inflammatory tissues. Many proteins have been described as receptors for "eat-me" signals presented by apoptotic cells, whereas others have been identified as involved in the formation of the phagocytic cup (52). The fact that efferocytic activity could be modulated by the macrophage activation state is highly important when seeking to design new therapeutic strategies targeting the resolution phase of inflammation as part of treatment for chronic inflammatory diseases (53). In our study, we identified the following proteins known to be induced in efferocytosis: CD14 (54), TGM2 (55), C1q (35), ALOX15 (56), ICAM1 (57), ITGAM (58).

Our results show that IL10/corticosteroid polarization is associated with a high efferocytic activity, related to overexpression of C1q (Fig. 7D). This protein is known to be a "bridging" molecule linking apoptotic cells (through calreticulin interaction) to receptors present on the macrophage membrane. One of these receptors is MerTK (supplemental Fig. S5), which is also expressed at the surface of IL10/DXM-

stimulated macrophages, and expression of which is at least partially controlled by C1q (36). Our results confirm, at the protein level, those of transcriptomic studies suggesting that C1q could be directly synthesized by macrophages in response to glucocorticoids (59). C1q is therefore responsible for controlling the expression of its own receptors, like MerTK, at the surface of macrophages. Data presented here also indicate that C1q is a molecular signature of M(IL10+DXM) macrophages associated with their high efferocytic activity and that its expression is unaffected by the environmental oxygen tension. ICAM1 (Inter Cellular Adhesion Molecule 1) has also been related to apoptotic cell clearance; it is downregulated by IL10/DXM stimulus. Downregulation of this protein is associated with activation of the PI3K/Akt signaling pathway, and with increased efferocytosis (57).

Transglutaminase 2 is a specific protein, the expression of which is controlled by IL-4. It has been presented as a biomarker of M(IL4+IL13) macrophages (39). This protein is also known to increase efferocytosis. Our results confirmed the specific expression of TGM2 in M(IL4+IL13) macrophages, but its expression was not associated with high efferocytosis levels. This result could be related to the fact that CD14 expression was downregulated in these macrophages. Indeed, CD14 is heavily involved in the clearance of apoptotic cells and has been described as necessary for the efferocytic activity of TGM2 (60). IL4/IL13 stimulation is also associated with downregulation of C1q (A fragment) expression. The ITGAM (CD11b/CD18) receptor, also known as CR3 (complement receptor 3), is overexpressed under IL4/IL13 and has been implicated in the clearance of opsonized apoptotic cells by iC3b. This process is inefficient when phagocytosis is performed with heat-inactivated serum (35), as it was the case in our study. Data presented here indicate that ALOX15 (Arachidonate 15-lipoxygenase) is specific to M(IL4+IL13) macrophages. This protein was significantly upregulated under 3% O_2 (Fig. 7A and 7B). However, low oxygen exposure alone is insufficient to induce its expression, as no expression was found in M(Ø) at 3% O_2 (Fig. 7A and 7B). This lipoxygenase is responsible for macrophage production of lipoxin A4, a substance which has been shown to increase efferocytosis (56). ALOX15 has also been implicated in orchestrating the clearance of apoptotic cells by causing oxidized products of phosphatidylethalonamine to be exposed on the plasma membrane of macrophages in which it is expressed. This effect increases the ability of these cells to internalize dead cells and inhibits their capture by inflammatory monocytes (61). This overexpression of ALOX15 was associated with a significant increase in efferocytic activity in macrophages polarized by IL4/IL13 under low environmental oxygen (Fig. 7D). This result reveals that a key function like the clearance of apoptotic cells is strongly related to both macrophage polarization and the surrounding physical microenvironment.

These results illustrate the importance of deciphering how the tissue context influences macrophage phenotype, not just

based on secreted biochemical signals. Our proteomic approach revealed the molecular signatures of many polarizations, and the effect of oxygen modulation on these signatures. The signatures themselves revealed many proteins involved in efferocytosis, and indicated how expression of these proteins is modulated by oxygen. This approach opens the way for the exploration of other environmental parameters as modulators of macrophage function and how these signals could be used to target these cells for therapeutic ends.

DATA AVAILABILITY

All MS proteomics data were deposited on the Proteome-Xchange Consortium website (http://proteomecentral.proteomexchange.org) via the PRIDE partner repository, data set identifier: PXD006354. Annotated spectra for identification of individual peptides are provided as supplemental data.

REFERENCES

1. Okabe, Y., and Medzhitov, R. (2016) Tissue biology perspective on macrophages. *Nat. Immunol.* **17,** 9–17
2. Wynn, T. A., Chawla, A., and Pollard, J. W. (2013) Macrophage biology in development, homeostasis and disease. *Nature* **496,** 445–455
3. Sica, A., and Mantovani, A. (2012) Macrophage plasticity and polarization: in vivo veritas. *J. Clin. Invest.* **122,** 787–795
4. Murray, P. J. (2017) Macrophage Polarization. *Annu. Rev. Physiol.* **79,** 541–566
5. Stein, M., Keshav, S., Harris, N., and Gordon, S. (1992) Interleukin 4 potently enhances murine macrophage mannose receptor activity: a marker of alternative immunologic macrophage activation. *J. Exp. Med.* **176,** 287–292
6. Martinez, F. O., and Gordon, S. (2014) The M1 and M2 paradigm of macrophage activation: time for reassessment. *F1000prime Rep.* **6,** 13
7. Sironi, M., Martinez, F. O., D'Ambrosio, D., Gattorno, M., Polentarutti, N., Locati, M., Gregorio, A., Iellem, A., Cassatella, M. A., Van Damme, J., Sozzani, S., Martini, A., Sinigaglia, F., Vecchi, A., and Mantovani, A. (2006) Differential regulation of chemokine production by Fcgamma receptor engagement in human monocytes: association of CCL1 with a distinct form of M2 monocyte activation (M2b, Type 2). *J. Leukoc. Biol.* **80,** 342–349
8. Chinetti-Gbaguidi, G., and Staels, B. (2011) Macrophage polarization in metabolic disorders: functions and regulation. *Curr. Opin. Lipidol.* **22,** 365–372
9. Chow, A., Brown, B. D., and Merad, M. (2011) Studying the mononuclear phagocyte system in the molecular age. *Nat. Rev. Immunol.* **11,** 788–798
10. Mosser, D. M., and Edwards, J. P. (2008) Exploring the full spectrum of macrophage activation. *Nat. Rev. Immunol.* **8,** 958–969
11. Murray, P. J., and Wynn, T. A. (2011) Protective and pathogenic functions of macrophage subsets. *Nat. Rev. Immunol.* **11,** 723–737
12. Ginhoux, F., Schultze, J. L., Murray, P. J., Ochando, J., and Biswas, S. K. (2015) New insights into the multidimensional concept of macrophage ontogeny, activation and function. *Nat. Immunol.* **17,** 34–40

13. Xue, J., Schmidt, S. V., Sander, J., Draffehn, A., Krebs, W., Quester, I., De Nardo, D., Gohel, T. D., Emde, M., Schmidleithner, L., Ganesan, H., Nino-Castro, A., Mallmann, M. R., Labzin, L., Theis, H., Kraut, M., Beyer, M., Latz, E., Freeman, T. C., Ulas, T., and Schultze, J. L. (2014) Transcriptome-based network analysis reveals a spectrum model of human macrophage activation. *Immunity* **40,** 274–288
14. Csete, M. (2005) Oxygen in the cultivation of stem cells. *Ann. N.Y. Acad. Sci.* **1049,** 1–8
15. Johansson, A., Lundborg, M., Sköld, C. M., Lundahl, J., Tornling, G., Eklund, A., and Camner, P. (1997) Functional, morphological, and phenotypical differences between rat alveolar and interstitial macrophages. *Am. J. Respir. Cell Mol. Biol.* **16,** 582–588
16. Pfau, J. C., Schneider, J. C., Archer, A. J., Sentissi, J., Leyva, F. J., and Cramton, J. (2004) Environmental oxygen tension affects phenotype in cultured bone marrow-derived macrophages. *Am. J. Physiol. Lung Cell. Mol. Physiol.* **286,** L354–L362
17. Grodzki, A. C. G., Giulivi, C., and Lein, P. J. (2013) Oxygen tension modulates differentiation and primary macrophage functions in the human monocytic THP-1 cell line. *PloS One* **8,** e54926
18. Elliott, M. R., and Ravichandran, K. S. (2016) The Dynamics of Apoptotic Cell Clearance. *Dev. Cell* **38,** 147–160
19. Murray, P. J., Allen, J. E., Biswas, S. K., Fisher, E. A., Gilroy, D. W., Goerdt, S., Gordon, S., Hamilton, J. A., Ivashkiv, L. B., Lawrence, T., Locati, M., Mantovani, A., Martinez, F. O., Mege, J.-L., Mosser, D. M., Natoli, G., Saeij, J. P., Schultze, J. L., Shirey, K. A., Sica, A., Suttles, J., Udalova, I., van Ginderachter, J. A., Vogel, S. N., and Wynn, T. A. (2014) Macrophage activation and polarization: nomenclature and experimental guidelines. *Immunity* **41,** 14–20
20. Kraut, A., Marcellin, M., Adrait, A., Kuhn, L., Louwagie, M., Kieffer-Jaquinod, S., Lebert, D., Masselon, C. D., Dupuis, A., Bruley, C., Jaquinod, M., Garin, J., and Gallagher-Gambarelli, M. (2009) Peptide storage: are you getting the best return on your investment? Defining optimal storage conditions for proteomics samples. *J. Proteome Res.* **8,** 3778–3785
21. Cox, J., Neuhauser, N., Michalski, A., Scheltema, R. A., Olsen, J. V., and Mann, M. (2011) Andromeda: a peptide search engine integrated into the MaxQuant environment. *J. Proteome Res.* **10,** 1794–1805
22. Cox, J., Hein, M. Y., Luber, C. A., Paron, I., Nagaraj, N., and Mann, M. (2014) Accurate proteome-wide label-free quantification by delayed normalization and maximal peptide ratio extraction, termed MaxLFQ. *Mol. Cell Proteomics* **13,** 2513–2526
23. Pathan, M., Keerthikumar, S., Ang, C.-S., Gangoda, L., Quek, C. Y. J., Williamson, N. A., Mouradov, D., Sieber, O. M., Simpson, R. J., Salim, A., Bacic, A., Hill, A. F., Stroud, D. A., Ryan, M. T., Agbinya, J. I., Mariadason, J. M., Burgess, A. W., and Mathivanan, S. (2015) FunRich: An open access standalone functional enrichment and interaction network analysis tool. *Proteomics* **15,** 2597–2601
24. Huang, D. W., Sherman, B. T., and Lempicki, R. A. (2009) Systematic and integrative analysis of large gene lists using DAVID bioinformatics resources. *Nat. Protoc.* **4,** 44–57
25. Vogel, D. Y. S., Glim, J. E., Stavenuiter, A. W. D., Breur, M., Heijnen, P., Amor, S., Dijkstra, C. D., and Beelen, R. H. J. (2014) Human macrophage polarization in vitro: maturation and activation methods compared. *Immunobiology* **219,** 695–703
26. Wuest, S. J. A., Crucet, M., Gemperle, C., Loretz, C., and Hersberger, M. (2012) Expression and regulation of 12/15-lipoxygenases in human primary macrophages. *Atherosclerosis* **225,** 121–127
27. Lee, C.-U., Song, E.-K., Yoo, C.-H., Kwak, Y.-K., and Han, M.-K. (2012) Lipopolysaccharide induces CD38 expression and solubilization in J774 macrophage cells. *Mol. Cells* **34,** 573–576
28. O'Shea, J. J., Gadina, M., and Schreiber, R. D. (2002) Cytokine signaling in 2002: new surprises in the Jak/Stat pathway. *Cell* **109,** S121–131
29. Lehtonen, A., Matikainen, S., and Julkunen, I. (1997) Interferons up-regulate STAT1, STAT2, and IRF family transcription factor gene expression in human peripheral blood mononuclear cells and macrophages. *J. Immunol.* **159,** 794–803
30. Platanias, L. C. (2005) Mechanisms of type-I- and type-II-interferon-mediated signalling. *Nat. Rev. Immunol.* **5,** 375–386
31. Newsholme, P., Curi, R., Gordon, S., and Newsholme, E. A. (1986) Metabolism of glucose, glutamine, long-chain fatty acids and ketone bodies by murine macrophages. *Biochem. J.* **239,** 121–125

32. Kelly, B., and O'Neill, L. A. J. (2015) Metabolic reprogramming in macrophages and dendritic cells in innate immunity. *Cell Res.* **25,** 771–784

33. Zanoni, I., Ostuni, R., Marek, L. R., Barresi, S., Barbalat, R., Barton, G. M., Granucci, F., and Kagan, J. C. (2011) CD14 controls the LPS-induced endocytosis of Toll-like receptor 4. *Cell* **147,** 868–880

34. Abrial, C., Grassin-Delyle, S., Salvator, H., Brollo, M., Naline, E., and Devillier, P. (2015) 15-Lipoxygenases regulate the production of chemokines in human lung macrophages. *Br. J. Pharmacol.* **172,** 4319–4330

35. Mevorach, D., Mascarenhas, J. O., Gershov, D., and Elkon, K. B. (1998) Complement-dependent clearance of apoptotic cells by human macrophages. *J. Exp. Med.* **188,** 2313–2320

36. Zizzo, G., Hilliard, B. A., Monestier, M., and Cohen, P. L. (2012) Efficient clearance of early apoptotic cells by human macrophages requires M2c polarization and MerTK induction. *J. Immunol.* **189,** 3508–3520

37. Martinez, F. O., Gordon, S., Locati, M., and Mantovani, A. (2006) Transcriptional profiling of the human monocyte-to-macrophage differentiation and polarization: new molecules and patterns of gene expression. *J. Immunol.* **77,** 7303–7311

38. Beyer, M., Mallmann, M. R., Xue, J., Staratschek-Jox, A., Vorholt, D., Krebs, W., Sommer, D., Sander, J., Mertens, C., Nino-Castro, A., Schmidt, S. V., and Schultze, J. L. (2012) High-resolution transcriptome of human macrophages. *PloS One* **7,** e45466

39. Martinez, F. O., Helming, L., Milde, R., Varin, A., Melgert, B. N., Draijer, C., Thomas, B., Fabbri, M., Crawshaw, A., Ho, L. P., Ten Hacken, N. H., Cobos Jiménez, V., Kootstra, N. A., Hamann, J., Greaves, D. R., Locati, M., Mantovani, A., and Gordon, S. (2013) Genetic programs expressed in resting and IL-4 alternatively activated mouse and human macrophages: similarities and differences. *Blood* **121,** e57–e69

40. O'Neill, L. A. J., and Pearce, E. J. (2016) Immunometabolism governs dendritic cell and macrophage function. *J. Exp. Med.* **213,** 15–23

41. Wolf, A., Agnihotri, S., Micallef, J., Mukherjee, J., Sabha, N., Cairns, R., Hawkins, C., and Guha, A. (2011) Hexokinase 2 is a key mediator of aerobic glycolysis and promotes tumor growth in human glioblastoma multiforme. *J. Exp. Med.* **208,** 313–326

42. Etienne, M. C., Chéradame, S., Fischel, J. L., Formento, P., Dassonville, O., Renée, N., Schneider, M., Thyss, A., Demard, F., and Milano, G. (1995) Response to fluorouracil therapy in cancer patients: the role of tumoral dihydropyrimidine dehydrogenase activity. *J. Clin. Oncol. Off. J. Am. Soc. Clin. Oncol.* **13,** 1663–1670

43. Janeway, C. A., Bottomly, K., Babich, J., Conrad, P., Conzen, S., Jones, B., Kaye, J., Katz, M., McVay, L., Murphy, D. B., and Tite, J. (1984) Quantitative variation in Ia antigen expression plays a central role in immune regulation. *Immunol. Today* **5,** 99–105

44. Ayala, A., Ertel, W., and Chaudry, I. H. (1996) Trauma-induced suppression of antigen presentation and expression of major histocompatibility class II antigen complex in leukocytes. *Shock* **5,** 79–90

45. Henze, A.-T., and Mazzone, M. (2016) The impact of hypoxia on tumor-associated macrophages. *J. Clin. Invest.* **126,** 3672–3679

46. Laoui, D., Van Overmeire, E., Di Conza, G., Aldeni, C., Keirsse, J., Morias, Y., Movahedi, K., Houbracken, I., Schouppe, E., Elkrim, Y., Karroum, O., Jordan, B., Carmeliet, P., Gysemans, C., De Baetselier, P., Mazzone, M., and Van Ginderachter, J. A. (2014) Tumor hypoxia does not drive differentiation of tumor-associated macrophages but rather fine-tunes the M2-like macrophage population. *Cancer Res.* **74,** 24–30

47. Conde, P., Rodriguez, M., van der Touw, W., Jimenez, A., Burns, M., Miller, J., Brahmachary, M., Chen, H., Boros, P., Rausell-Palamos, F., Yun, T. J., Riquelme, P., Rastrojo, A., Aguado, B., Stein-Streilein, J., Tanaka, M., Zhou, L., Zhang, J., Lowary, T. L., Ginhoux, F., Park, C. G., Cheong, C., Brody, J., Turley, S. J., Lira, S. A., Bronte, V., Gordon, S., Heeger, P. S., Merad, M., Hutchinson, J., Chen, S.-H., and Ochando, J. (2015) DC-SIGN(+) Macrophages Control the Induction of Transplantation Tolerance. *Immunity* **42,** 1143–1158

48. Geijtenbeek, T. B. H., and Gringhuis, S. I. (2009) Signalling through C-type lectin receptors: shaping immune responses. *Nat. Rev. Immunol.* **9,** 465–479

49. Tailleux, L., Pham-Thi, N., Bergeron-Lafaurie, A., Herrmann, J.-L., Charles, P., Schwartz, O., Scheinmann, P., Lagrange, P. H., de Blic, J., Tazi, A., Gicquel, B., and Neyrolles, O. (2005) DC-SIGN Induction in Alveolar Macrophages Defines Privileged Target Host Cells for Mycobacteria in Patients with Tuberculosis. *PLoS Med.* **2,**

50. Roszer, T., Menéndez-Gutiérrez, M. P., Lefterova, M. I., Alameda, D., Núñez, V., Lazar, M. A., Fischer, T., and Ricote, M. (2011) Autoimmune kidney disease and impaired engulfment of apoptotic cells in mice with macrophage peroxisome proliferator-activated receptor gamma or retinoid X receptor alpha deficiency. *J. Immunol.* **186,** 621–631

51. Hu, Z., Zhou, Q., Zhang, C., Fan, S., Cheng, W., Zhao, Y., Shao, F., Wang, H.-W., Sui, S.-F., and Chai, J. (2015) Structural and biochemical basis for induced self-propagation of NLRC4. *Science* **350,** 399–404

52. Devitt, A., and Marshall, L. J. (2011) The innate immune system and the clearance of apoptotic cells. *J. Leukoc. Biol.* **90,** 447–457

53. Fullerton, J. N., and Gilroy, D. W. (2016) Resolution of inflammation: a new therapeutic frontier. *Nat. Rev. Drug Discov.* **15,** 551–567

54. Devitt, A., Moffatt, O. D., Raykundalia, C., Capra, J. D., Simmons, D. L., and Gregory, C. D. (1998) Human CD14 mediates recognition and phagocytosis of apoptotic cells. *Nature* **392,** 505–509

55. Tóth, B., Garabuczi, E., Sarang, Z., Vereb, G., Vámosi, G., Aeschlimann, D., Blaskó, B., Bécsi, B., Erdődi, F., Lacy-Hulbert, A., Zhang, A., Falasca, L., Birge, R. B., Balajthy, Z., Melino, G., Fésüs, L., and Szondy, Z. (2009) Transglutaminase 2 is needed for the formation of an efficient phagocyte portal in macrophages engulfing apoptotic cells. *J. Immunol.* **182,** 2084–2092

56. Godson, C., Mitchell, S., Harvey, K., Petasis, N. A., Hogg, N., and Brady, H. R. (2000) Cutting edge: lipoxins rapidly stimulate nonphlogistic phagocytosis of apoptotic neutrophils by monocyte-derived macrophages. *J. Immunol.* **164,** 1663–1667

57. Yang, M., Liu, J., Piao, C., Shao, J., and Du, J. (2015) ICAM-1 suppresses tumor metastasis by inhibiting macrophage M2 polarization through blockade of efferocytosis. *Cell Death Dis.* **6,** e1780

58. Takizawa, F., Tsuji, S., and Nagasawa, S. (1996) Enhancement of macrophage phagocytosis upon iC3b deposition on apoptotic cells. *FEBS Lett.* **397,** 269–272

59. Ehrchen, J., Steinmüller, L., Barczyk, K., Tenbrock, K., Nacken, W., Eisenacher, M., Nordhues, U., Sorg, C., Sunderkötter, C., and Roth, J. (2007) Glucocorticoids induce differentiation of a specifically activated, anti-inflammatory subtype of human monocytes. *Blood* **109,** 1265–1274

60. Eligini, S., Fiorelli, S., Tremoli, E., and Colli, S. (2016) Inhibition of transglutaminase 2 reduces efferocytosis in human macrophages: Role of CD14 and SR-AI receptors. *Nutr. Metab. Cardiovasc. Dis.* **26,** 922–930

61. Uderhardt, S., Herrmann, M., Oskolkova, O. V., Aschermann, S., Bicker, W., Ipseiz, N., Sarter, K., Frey, B., Rothe, T., Voll, R., Nimmerjahn, F., Bochkov, V. N., Schett, G., and Krönke, G. (2012) 12/15-lipoxygenase orchestrates the clearance of apoptotic cells and maintains immunologic tolerance. *Immunity* **36,** 834–846